Technical Report: Scalable Video Multicast in Hybrid 3G/Ad-hoc Networks

Sha Hua*, Yang Guo†, Yong Liu*, Hang Liu†, Shivendra S. Panwar*
*Department of Electrical and Computer Engineering,
Polytechnic Institute of New York University, Brooklyn, NY 11201
Emails: shua01@students.poly.edu; yongliu@poly.edu; panwar@catt.poly.edu
†2 Independence Way,
Technicolor Corporate Research, Princeton, NJ 08540
Emails: {Yang.Guo, Hang.Liu}@technicolor.com

Abstract

Mobile video broadcasting service, or mobile TV, is expected to become a popular application for 3G wireless network operators. Most existing solutions for video Broadcast Multicast Services (BCMCS) in 3G networks employ a single transmission rate to cover all viewers. The system-wide video quality of the cell is therefore throttled by a few viewers close to the boundary, and is far from reaching the social-optimum allowed by the radio resources available at the base station. In this paper, we propose a novel scalable video broadcast/multicast solution, **SV-BCMCS**, that efficiently integrates scalable video coding, 3G broadcast and ad-hoc forwarding to balance the system-wide and worst-case video quality of all viewers at 3G cell. We solve the optimal resource allocation problem in SV-BCMCS and develop practical helper discovery and relay routing algorithms. Moreover, we analytically study the gain of using ad-hoc relay, in terms of users' effective distance to the base station. Through extensive real video sequence driven simulations, we show that SV-BCMCS significantly improves the system-wide perceived video quality. The users' average PSNR increases by as much as 1.70 dB with slight quality degradation for the few users close to the 3G cell boundary.

Index Terms

Scalable Video Coding, Resource Allocation, Ad-hoc Video Relay,

EDICS Category

5-WRLS (Wireless Multimedia Communication)

I. Introduction

User demands for content-rich multimedia are driving much of the innovation in wireline and wireless networks. Watching a movie or a live TV show on their cell phones, at anytime and at any place, is an attractive application to many users. Mobile video broadcasting service, or mobile TV, is expected to become a popular application for 3G network operators. The service is currently operational, mainly in the unicast mode, with individual viewers assigned to dedicated radio channels. However, a unicast-based solution is not scalable. A Broadcast/Multicast service over cellular networks is a more efficient solution with the benefits of low infrastructure cost, simplicity in integration with existing voice/data services, and strong interactivity support. Thus, it is a significant part of 3G cellular service. For instance, Broadcast/Multicast Services (BCMCS) [1], [2] has become a part of the standards in the Third Generation Partnership Project 2 (3GPP2) [3] for providing broadcast/multicast service in the CDMA2000 setting. However, most existing BCMCS solutions employ a single transmission rate to cover all viewers, regardless of their locations in the cell. Such a design is sub-optimal. Viewers close to the base-station are significantly "slowed down" by viewers close to the cell boundary. The system-wide perceived video quality is far from reaching the social-optimum.

In this paper, we propose a novel scalable video broadcast/multicast solution, **SV-BCMCS***, that efficiently integrates scalable video coding, 3G broadcast and ad-hoc forwarding to achieve the optimal trade-off between the system-wide and worst-case video quality perceived by all viewers in the cell.* In our solution, video is encoded into one base layer and multiple enhancement layers using Scalable Video Coding (SVC) [4]. Different layers are broadcast at different rates to cover viewers at different ranges. To provide the basic video service to all viewers, the base layer is always broadcast to the entire cell. The channel resources/bandwidth of the enhancement layers are optimally allocated to maximize the system-wide video quality given the locations of the viewers and radio resources available at the base station. In addition, we allow viewers to forward enhancement layers to each other using short-hop and high-rate ad-hoc connections. In summary, the major contribution of this paper is as follows:

1) We study the optimal resource allocation problem for scalable video multicast in 3G networks. We show that the system-wide video quality can be significantly increased by jointly assigning the channel resources for enhancement layers. Our solution strikes a good balance between the average and worst-case performance for all viewers in the cell.
2) For ad-hoc video forwarding, we design an efficient helper discovery scheme for viewers to obtain additional enhancement layers from their ad-hoc neighbors a few hops away. Also a multi-hop relay routing scheme is designed to exploit the broadcast nature of ad-hoc transmissions and eliminate redundant video relays from helpers to their receivers.

3) We develop analytical models to study the expected gain of few-hop ad-hoc video relays under random user distribution in a 3G cell. An ad-hoc relay shortens the effective distance of the user to the base station, which is crucial to the throughput improvement of wireless transmission. Based on the models, we give the mathematical solution for the effective distance gain. The analysis underpins our protocol design from a theoretical viewpoint.
4) We selected three representative video sequences, and conducted video trace driven simulations using OPNET. We systematically evaluated the performance improvement attributed to several important factors, including node density, the number of relay hops, user mobility and coding rates of video layers. Simulations show that SV-BCMCS significantly improves the video quality perceived by users in practical 3G/ad-hoc hybrid networks.

The rest of the paper is organized as follows. Related work is described in Section II. The SV-BCMCS architecture is first introduced in Section III. We then formulate the optimal layered video broadcast problem and present a dynamic programming algorithm to solve it. Following that, we develop the helper discovery and multiple-hop relay routing algorithms. We develop analytical models to study the expected gain of few-hop ad-hoc video relay in Section IV. Video trace driven simulation results are shown and discussed in Section V. The paper is concluded in Section VI.

II. Related Work

Using ad-hoc links to help data transmissions in 3G networks has been studied by several research groups in the past. In [5], a Unified Cellular and Ad-hoc Network (UCAN) architecture for enhancing cell throughput has been proposed, which is the starting point of our work. Clients with poor channel quality select clients with better channel quality as their proxies to receive data from the 3G base station. A packet to a client is first sent by the base station to its proxy node through a 3G channel. The proxy node then forwards the packet to the client through an ad-hoc network composed of other mobile clients and IEEE 802.11 wireless links. In [6], the authors discovered the reason for the inefficiency that arises when using an ad-hoc peer-to-peer network as-is in a cellular system. Then they proposed two approaches to improve the performance, one is to leverage assistance from the base station, and the other is to leverage the relaying capability of multi-homed hosts.

While the above articles are focused on the unicast data transmission in cellular networks, ad-hoc transmission can be also employed to improve the performance of 3G Broadcast/Multicast Services. Based on the UCAN, Park and Kasera [7] developed a new proxy discovery algorithm for the cellular multicast receivers. The effect of ad-hoc path interference is taken into consideration. ICAM [8] developed a close-to-optimal algorithm for the construction of the multicast forest for the integrated cellular and ad-hoc network. Sinkar et al. [9] proposed a novel method to provide QoS support by using an ad-hoc assistant network to recover the loss of multicast data in the cellular network. However, the aforementioned works did not make use of SVC coded streams, which allow cellular operators to flexibly select the operating point so as to strike the right balance between the system-wide aggregate performance and individual users' perceived video quality.

Layered video multicasting combined with adaptive modulation and coding to maximize the video quality in an infrastructure based wireless network is studied in [10]–[12]. They differ in the formulation of the optimal resource allocation problem. Peilong et al. [13] and Donglin et al. [14] extended this idea into multi-carrier and cognitive radio scenarios. None of them, however, takes the advantage of the assistance of ad-hoc networks. Our work is also relevant to the studies of scalable video transmission over pure ad-hoc networks such as [15]. The authors in [15] consider the scenario of scalable video streaming from multiple sources to multiple users. A distributed scheme that optimizes the rate-distortion is introduced. In contrast, this paper studies the scalable video streaming in the 3G networks with the assistance of ad-hoc network formed among users' mobile devices. The optimization problem is solved at the 3G base station. The distributed relay routing protocol is designed to locate the helping devices. Finally, the current paper substantially extends the preliminary version of our results which appeared in [16]. The analytical models are developed to study the expected gain of ad-hoc video relays under a random user distribution. PSNR, instead of received video rate, is used as the target function in the optimization problem and in the simulation experiments, which better reflects the users' perceived video quality. In addition, real video trace driven simulations are conducted to evaluate the system performance.

III. Scalable Video Broadcast/Multicast Service (SV-BCMCS) over a Hybrid Network

In this section, we start with the introduction of the SV-BCMCS architecture. We then formulate and solve the optimal resource allocation problem for the base station to broadcast scalable video with the aid of an ad-hoc network. Finally, we develop the helper discovery and layered video relay routing algorithms to explore the performance improvement introduced by ad-hoc connections between viewers.

A. System Architecture

In SV-BCMCS, through SVC coding, video is encoded into one base layer and multiple enhancement layers. Viewers who receive the base layer can view the video with the minimum quality. The video quality improves as the number of received layers increases. An enhancement layer can be decoded if and only if all enhancement layers below it are received. The multicast radio channel of the base station is divided into multiple sub-channels. Here a sub-channel stands for either a temporal or

TABLE I
NOTATION USED IN THIS PAPER

r_i	selected transmission rate (PHY mode) for layer i video content
p_i	allocated fraction of channel for tansmission of layer i video content in 3G system
n_i	number of multicast users that can receive layer i video/content in 3G domain
R_i	encoding rate of an individual layer i.
L	total number of layers
N	total number of multicast users in the 3G domain
$\mathcal{N}$	the set of multicast users in the 3G domain. $\|\mathcal{N}\| = N$
Φ	set of all possible transmission rates (or PHY modes)
U_{total}	aggregate utility of users in the 3G domain
d	distance of the user to the base station
r_t	ad-hoc transmission radius/range for each user
G	random variable of effective distance gain
S_c	total area of the entire 3G cell
D	the radius of the 3G cell

frequency division of the bandwidth. Different layers of video are broadcast using different sub-channels with different coverage ranges. To maintain the minimum quality for all viewers, the base layer is always broadcast using a sub-channel to cover the entire cell. To address the decoding dependency of upper layers on lower layers, the broadcast range of lower layers cannot be shorter than that of the higher layers.

Figure 1 depicts the system architecture of SV-BCMCS as with eleven multicast users and three layers of SVC video, denoted by $L1$, $L2$, and $L3$. The base station broadcasts three layers using three sub-channels with their respective coverage areas shown in the figure. All the users receive $L1$ from the base station directly, while four users receive $L2$ and two users receive $L2$ and $L3$ as well. With an ad-hoc network, the coverage of enhancement layers is extended further. As an example, user a is in the coverage of $L3$ and user b is in the coverage of $L2$. User a relays $L3$ to user b, who then relays $L3$ to users c and d. Meanwhile, user b relays $L2$ to users c and d. Effectively, all four users a, b, c, and d receive all three layers through the combinations of base station broadcast and ad-hoc relays.

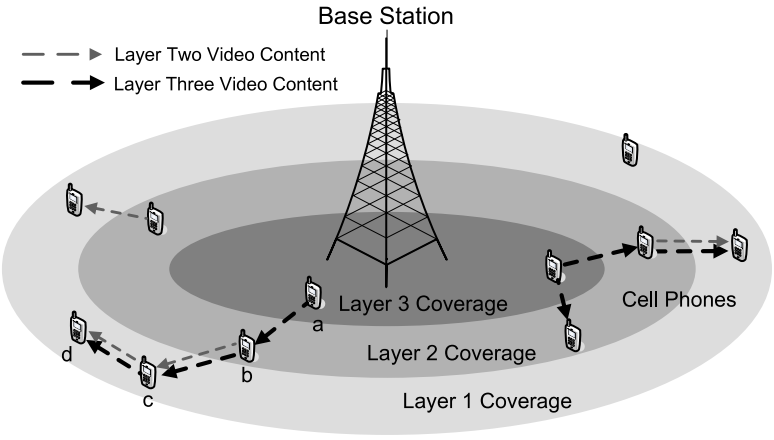

Fig. 1. Architecture of SV-BCMCS over a hybrid network (assuming three layers of video content).

The key design questions of the SV-BCMCS architecture are:

1) How to allocate the radio resources among sub-channels to different video layers to strike the right balance between system-wide and worst-case video quality among all users?
2) How to design an efficient helper discovery and relay routing protocol to maximize the gain of ad-hoc video forwarding?

We examine these questions through analysis and simulations in the following sections. The key notation used in this paper are shown in Table I.

B. Optimal Resouce Allocation in Layered Video Multicast

Our objective for radio resource allocation is to maximize the aggregate user perceived video quality while providing the base-line minimum quality service for all users. The perceived video quality can be measured by PSNR (Peak Signal-to-Noise Ratio) or distortion, with PSNR $= 10\log_{10}(M_I^2/D)$ (D is the distortion represented by the MSE (Mean Square Error) between the original image and the reconstructed image, and M_I is the maximum pixel value, typically set to be 255). The PSNR or distortion of a video sequence is the average of the corresponding measurements over all images in the same video sequence.

Modeling the distortion or the PSNR as the function of the user's received data rate is an ongoing research topic. For example, in [17], distortion is modeled as a continuous function of video rate. In [15], the distortion with SVC is modeled as discrete values depending on the number of layers received by the user. In [18] and [19], PSNR is modeled as a linear/piece-wise linear function of the video rate with SVC. Here we employ a general non-decreasing utility function $U(R^{rec})$ in the optimization formulation, with R^{rec} being a user's receiving data rate. In Section V, we replace the general utility function by a video sequence's actual PSNR values.

Assume there are L video layers, and the video rate of each layer is a constant R_i, $1 \le i \le L$. The broadcast channel is divided into L sub-channels through time-division multiplexing. Each sub-channel can operate at one of the available BCMCS PHY modes. Each PHY mode has a constant data transmission rate and a corresponding coverage range. Layer i is transmitted using sub-channel i. Let p_i be the time fraction allocated to sub-channel i, and r_i be the actual transmission rate, or the PHY mode, employed by sub-channel i. In practice, to support the video rate R_i of layer i, $r_i \cdot p_i \ge R_i$. We let $p_i = \frac{R_i}{r_i}$ in our formulation. In addition, the summation of the time fractions must be less than one $\sum_{i=1}^{L} p_i \le 1$.

Suppose n_i multicast users can receive the i-th layer video. Therefore $n_i - n_{i-1}$ users, $1 \le i < L$, receive i layers of video, while n_L users receive all L layers. The aggregate utility for all users is:

$$\begin{aligned} U_{total} &= \sum_{i\in\mathcal{N}} U(R_i^{rec}) \\ &= (n_1 - n_2)\cdot U(R_1) + \cdots + (n_j - n_{j+1})\cdot U(\sum_{i=1}^{j} R_i) + \cdots + n_L \cdot U(\sum_{i=1}^{L} R_i) \\ &= \sum_{i=1}^{L} (n_i - n_{i+1}) U(\sum_{j=1}^{i} R_j). \end{aligned} \tag{1}$$

with $n_{L+1} = 0$. For a fixed total number of multicast users N in the 3G domain, maximizing the average utility of multicast users is the same as maximizing the aggregate utility U_{total} in Eqn. (1).

Next, the computation of n_i is discussed. Let's first consider the base station transmission part. The number of users that can receive layer i directly from the base station is determined by the transmission rate r_i for sub-channel i (specifically, determined by the receiving SNR for the PHY mode with rate r_i). We can define this number of users as $f_{BS}(r_i)$ for layer i. Due to path loss, fading, and user mobility, $f_{BS}(r_i)$ varies with r_i and generally is a monotonically decreasing function of r_i. Namely the higher the transmission rate of the base station, the fewer the multicast users that can achieve the receiving SNR requirement and thus correctly receive the data.

In the second step, we take the ad-hoc relay into consideration. In SV-BCMCS, users who cannot receive layer i from the base station directly may receive it through the ad-hoc network. We use $f_{AD-HOC}(r_i)$ to denote the number of users obtaining the layer i video through ad-hoc relay from other users. Thus $n_i = f(r_i) = f_{BS}(r_i) + f_{AD-HOC}(r_i)$. In the system design, the base station gathers information about which user is getting data from which helper to compute n_i. This is done in the helper discovery protocol illustrated in Section III-D.

The optimal radio resource allocation problem can be formulated as the following utility maximization problem:

$$\max_{\{r_i\}} \quad U_{total} = \sum_{i=1}^{L} [f(r_i) - f(r_{i+1})] U(\sum_{j=1}^{i} R_j), \tag{2}$$

subject to:

$$r_i \le r_j \qquad i \le j \text{ and } i, j = 1, 2, \cdots L, \tag{3}$$

$$\sum_{i=1}^{L} (\frac{R_i}{r_i}) \le 1, \tag{4}$$

$$f(r_1) = N, \tag{5}$$

$$r_i \in \Phi. \tag{6}$$

The objective is to find a set of transmission rates r_i for individual layers so as to maximize the aggregate utility. The constraint given by (3) ensures that the coverage of lower layers is larger than that of the higher layers. Constraint (4) guarantees the

sum of sub-channels is no greater than the original channel. Constraint (5) ensures that the base layer covers the whole cell to provide basic video service to all the users. Finally, Φ is the set of possible transmission rates (or PHY modes). Note that the traditional broadcast/multicast with one single stream is a special case of the above optimization problem with $L = 1$.

C. Dynamic Programming Algorithm

The optimization problem formulated above can be solved by a dynamic programming algorithm. To facilitate the design of the dynamic programming algorithm, a time unit of the original channel is divided into K equal length time slots. Sub-channel i broadcasts the i-th layer of rate R_i, which requires $\lceil \frac{R_i}{r_i} \cdot K \rceil$ time slots. It is desireable that $\{\frac{R_i}{r_i} \cdot K\}$ are integers so as to avoid the channel bandwidth wastage. This can be achieved by selecting K to be 10^n where the fraction numbers $\{\frac{R_i}{r_i}\}$ are represented using at most n significant digits.

The objective function shown in Eqn. (2) can be transformed as:

$$U_{total} = \sum_{i=1}^{L} [f(r_i) - f(r_{i+1})] U(\sum_{j=1}^{i} R_j) = \sum_{i=1}^{L} f(r_i)[U(\sum_{j=1}^{i} R_j) - U(\sum_{j=1}^{i-1} R_j)], \tag{7}$$

with $U(\sum_{j=1}^{i-1} R_j) = 0$ for $i = 1$. Transmitting the ith layer with rate r_i contributes a utility gain of $f(r_i)[U(\sum_{j=1}^{i} R_j) - U(\sum_{j=1}^{i-1} R_j)]$ to the total utility U_{total}. Define S_i^k to be the transmission rate of the ith layer that gives the maximal utility gain using no more than k time slots, and U_i^k to be the corresponding maximum utility gain. We have

$$S_i^k = \min\{r_i \in \Phi \cup \{\infty\} \mid \frac{R_i}{r_i} K \le k\}, \tag{8}$$

$$U_i^k = f(S_i^k) \cdot [U(\sum_{j=1}^{i} R_j) - U(\sum_{j=1}^{i-1} R_j)] \qquad \forall 1 \le i \le L. \tag{9}$$

Since $f(r_i)$ is a non-increasing function, smaller r_i leads to greater $f(r_i)$. Given the number of time slots k, r_i should be the smallest PHY mode in Φ that can broadcast i-th layer. In case the value of k is too small and no PHY mode in Φ can satisfy the condition of $\frac{R_i}{r_i} K \le k$, the i-th layer cannot be broadcasted. The value of S_i^k is set to be ∞. We let $f(\infty) = 0$ and the correspondingly U_i^k to be zero.

We further define $\mathcal{U}_i^k$ to be the maximal utility gain of transmitting the first i layers (from layer 1 to layer i) with the aggregate number of time slots no greater than k, and define $\mathcal{S}_i^k$ to be the corresponding transmission rate vector for the first i layers. The dynamic programming algorithm is illustrated in **Algorithm 1** with $\mathcal{U}_L^K$ giving the optimal solution.

Algorithm 1 Dynamic programming algorithm for sub-channel resource allocation problem

1: **for** k = 1 to K **do**
2: $\quad \mathcal{U}_1^k = U_1^k$
3: $\quad \mathcal{S}_1^k = \{S_1^k\}$
4: **end for**
5: **for** i = 2 to L **do**
6: $\quad$ **for** k = 1 to K **do**
7: $\quad\quad m^* = \arg\max_{\{m \in [1,k] \text{ and } \mathcal{S}_{i-1}^m[i-1] \le S_i^{k-m}\}} \{\mathcal{U}_{i-1}^m + U_i^{k-m}\}$
8: $\quad\quad \mathcal{U}_i^k = \mathcal{U}_{i-1}^{m^*} + U_i^{k-m^*}$
9: $\quad\quad \mathcal{S}_i^k = \mathcal{S}_{i-1}^{m^*} \cup \{S_i^{k-m^*}\}$
10: $\quad$ **end for**
11: **end for**
12: return $\mathcal{U}_L^K$, $\mathcal{S}_L^K$

In the above algorithm, line 5 to line 11 updates $\mathcal{U}_i^k$ to include a new layer at each iteration. Line 7 and 8 solves the maximal utility problem of $\mathcal{U}_i^k$. Line 9 expands the transmitting rate vector $\mathcal{S}_L^k$ by appending the optimal transmitting rate of layer i. Condition $\mathcal{S}_{i-1}^m[i-1] \le S_i^{k-m}$ in line 7 ensures that the broadcasting ranges of the higher layers are no greater than the lower layers, satisfying the Constraint (3). Note the algorithm is for a general problem without considering Constraint (5). If Constraint (5) is in effect, we can replace the K in line 6 with $K' = K(1 - \frac{R_1}{r_1})$, where r_1 is the highest rate in Φ that can cover the entire cell (highest rate of r_i uses the least number of time slots). Then we solve the optimization problem with $L - 1$ layers, i.e., from layers 2 to L. The maximum utility is $f(r_1) \cdot U(R_1) + \mathcal{U}_{L-1}^{K'}$. The complexity of the algorithm is $O(LK^2)$.

D. Ad-hoc Video Relay: Helper Discovery and Relay Routing

In a pure SV-BCMCS solution, users closer to the base station will receive more enhancement layers from the base station. They can forward those layers to users further away from the base station through ad-hoc links. Ad-hoc video relays are done in two steps: 1) each user finds a helper in its ad-hoc neighborhood to download additional enhancement layers; 2) helpers merge download requests from their clients and forward enhancement layers through local broadcast.

1) Greedy Helper Discovery Protocol: We design a greedy protocol for users to find helpers. A greedy helper discovery protocol in the 3G and ad-hoc hybrid network was first presented in [5]. In that paper every node of the multicast group maintains a list of its neighbors, containing their IDs and the average 3G downlink data rates within a time window. Users periodically broadcast their IDs and downlink data rates to their neighbors. Each user greedily selects a neighbor with the highest downlink rate as its helper. Whenever a node wants to download data from the base station, it initiates helper discovery by unicasting a request message to its helper. Then the helper will forward this message to its own helper, so on and so forth, until the ad-hoc hop limit is reached or a node with the local maximum data rate is found. The ad-hoc hop limit is set by a parameter called Time-To-Live (TTL). The base station will send the data to the last-hop helper. The helpers will forward the data in the reverse direction of helper discovery to the requesting node.

We employ a similar greedy helper discovery mechanism. But unlike the case considered in [5], the locations and average 3G downlink data rates of helpers will affect the resource allocation strategy of the base station in SV-BCMCS. In our scheme, the last-hop node in the path sends the final request message to the base station. Upon receiving this message, the base station updates the 3G data rate information of all the nodes along the path as the last-hop node's 3G rate, assuming the ad-hoc link throughput is much larger than the 3G data rate. After that, the base station might resolve the coverage function as $f(r_i) = \{\text{Number of nodes with updated 3G rate above } r_i\}$. The optimal broadcast strategy can then be calculated by solving the optimization problem defined in (2).

Moreover, to facilitate efficient relay routing, a node also needs to keep information about the relay requests routed through itself. The last-hop helper in the path also sends the final request message back to the initiating node. Every user along this ad-hoc path will get a copy of this final message.

As an example, the whole process is shown in Figure 2. User C attempts to find a helper within two hops to improve its video quality. Its request goes through B to A. E and F are ignored by C and B, since they are not the neighbor with highest 3G rate. To this end, User A knows where user C is located by the reverse route of the path that user C followed to find user A. User A sends the request message to the base station to indicate that user A will act as user C's helper using the relay path along user B. Meanwhile, User A also sends this message (confirmation message) back to user C confirming that user A will act as its helper.

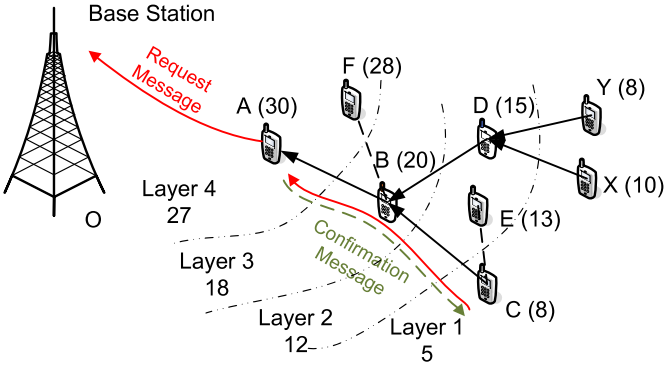

Fig. 2. Greedy Helper Discovery Protocol and Relay Routing Protocol. The numbers in parenthesis are the average 3G rates for each node. The dashed line indicates the ad-hoc neighborhood. The straight solid line is the ad-hoc path with the arrow pointing to the helper. For relay routing protocol, dashed-dotted lines represent the coverage area of each layer. 27, 18, 12 and 5 are the physical transmission rates for layers 4, 3, 2 and 1.

Note that [5] also proposed another helper discovery protocol using flooding. Instead of unicast, each node broadcasts the request message hop by hop. This method enables a node to find the helper with the global maximum data rate within the ad-hoc hop limit range. However, considering the large overhead of flooding messages in the ad-hoc network, we only adopt the greedy helper discovery protocol within the SV-BCMCS context.

2) SV-BCMCS Relay Routing Protocol: The SV-BCMCS routing protocol runs after the greedy helper selection protocol and the optimal radio resource allocation. Assuming optimal radio resource allocation has been performed, the base station decides to transmit the L layers with different rates $r_1, r_2, \cdots, r_L$. It will broadcast this information to every node in the cell. Moreover, in the greedy helper discovery phase, each node obtains the information for all the relay paths to which it belongs. The major goal of the relay routing protocol is to maximally exploit the broadcast nature of ad-hoc transmissions and merge multiple relay requests for the same layer on a common helper.

Essentially, each helper needs to locally determine which received layers will be forwarded to its requesting neighbors. For each node n, define the set $\mathcal{K}$ ={all neighbors that use n as one-hop helper}, the forwarding decision will be calculated distributedly as shown in Algorithm2.

Algorithm 2 Forwarding Algorithm in SV-BCMCS Routing Protocol for Node n

$\mathcal{K}$ ={all neighbors that use n as one-hop helper }
for $k \in \mathcal{K}$ **do**
  Find the highest layer l_k that k can directly receive from the base station
  Find the highest layer L_k that k can expect from any potential helper
end for
$l_{min} = \min\{l_k, k \in \mathcal{K}\}$
$L_{max} = \max\{L_k, k \in \mathcal{K}\}$
node n broadcasts the packets between layer $l_{min} + 1$ to L_{max} to its one-hop neighbors.

For the receiving part, each node receives packets that satisfy two conditions: (i) the packets are sent from its direct one-hop helper; (ii) the packets belong to a layer that the node cannot directly receive from the base station. Otherwise the node will discard the packets. That is, the node has no use for packets that are within the layer to which the node belongs, or from a lower layer than the layer to which it belongs.

A relay routing example is illustrated in Figure 2. Suppose $L = 4$ and maximal hop number (TTL) is 2. For node B in the figure, nodes C and D use it as a direct one-hop helper. For D, $l_D = 2$ (it is the layer to which node D belongs) according to the figure, and within 2 hops, D's highest expected layer is $L_D = 4$. The highest expected layer is the highest layer which a node can expect to receive through its helpers while constrained by the TTL. In the same way, we can derive, $l_C = 1$ and $L_C = 4$. Thus, for node B, $l_{min} = \min\{l_C, l_D\} = 1$ and $L_{max} = \max\{L_C, L_D\} = 4$. Therefore, node B will broadcast the packets in layers 2, 3 and 4. Since node D is in layer 2, it will receive packets from node B in layers 3 and 4 only. Meanwhile, node C will receive all the packets in layers 2, 3 and 4.

Note a local broadcast doesn't use RTS/CTS exchange in a practical implementation based on IEEE 802.11. Instead, the nodes' carrier sensing threshold can be set to a reasonable small value. In this way, we can reduce the number of collisions due to hidden terminal problem while still keep a favorable spatial reuse factor in the network.

In practice, wireless channels are error-prone and link quality changes over time due to the fading and interference. This poses a challenge particularly to the video transmission. Due to the use of spatial temporal prediction, a compressed video is susceptible to transmission errors. To overcome such problem, appropriate error protection mechanism is necessary in the practical implementation. FEC (Forward Error Correction) is widely used as an effective means to combat packet losses over wireless channel [15], [20], [21], Our relay routing protocol can be easily extended to support FEC by letting the helper nodes decode and re-generate the parity packets for each video layer before forwarding them. We will evaluate the performance of our system with FEC in Section V.

IV. Analysis of the Gain of Ad-hoc Relay

In this section, we analytically study the expected gain from using ad-hoc relays under a random node distribution in the cell. Through ad-hoc video relays, users receiving fewer layers of packets (users at the coverage edge/boundary) are able to obtain video/content layers that they otherwise would not or could not receive. From the base station's viewpoint, an ad-hoc relay shortens a user's *effective distance* to the base station. As shown in Figure 2, user A relays data to user B who then relays the data to user C. If we assume that the bandwidth of an ad-hoc link is much larger than the 3G multicast rate, both user B and C can be seen as located at the same place as user A, then have the same effective distance as user A.

We define the *distance gain* of a user as the difference between its original distance to the base station and its last helper's distance to the base station. For example, the distance gain of user C is the difference between $\overline{OC}$ and $\overline{OA}$, where O denotes the position of the base station. We are particularly interested in this metric due to the fact that in wireless communications, the distance between the transmitter and the receiver fundamentally affects their transmission rate. In the following, we develop a probabilistic model to study the distance gain due to ad-hoc relays under a random node distribution. Note that such distance gain is an upper bound to the case with limited ad-hoc bandwidth, which is able to show the insight of benefits brought by ad-hoc relay.

The typical transmission rate of an ad-hoc network, such as a network using IEEE 802.11, is much larger than the rate of a cellular network. For instance, IEEE 802.11g supports data rates up to 54 Mb/s. We therefore ignore the effect of wireless interference in our analysis. The interference will be included in our OPNET based simulation in the next section. We also assume that the number of data relays, or relay hops, is small. Using only a small number of relays is more robust against user mobility, and reduces the video forwarding delay. Furthermore, a smaller number of relays also reduces the traffic volume in the whole ad-hoc network.

Let G be the distance gain of an arbitrary user. Obviously, G depends on the location of the user, as well as the locations of other users in the same cell. It is also a function of the ad-hoc transmission range, and the number of relay hops allowed. Denote by $f_G(\cdot)$ the probability density function (pdf) of G. We develop a model to characterize $f_G(\cdot)$ by assuming the users are uniformly distributed in the cell. Our approach, however, also applies to other distributions within the cell. The list of key notation is included in Table I. Figure 4 depicts an arbitrary user and is used to study the user's distance gain in the case of a one-hop and two-hop relay.

A. Distance Gain Using One-hop Relay

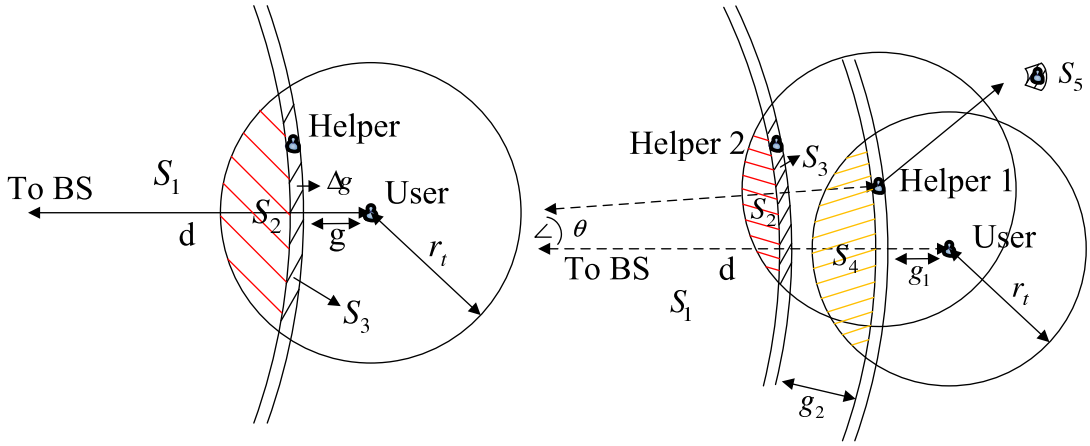

Fig. 3. The one-hop(left) and two-hop(right) ad-hoc relay analysis for an arbitrary user.

Assuming that the user is d distance away from the base station, and the ad-hoc transmission radius/range is r_t. All other users falling into the transmission range of the user are potential one-hop helpers. Following the greedy helper discovery protocol, the user closest to the base station is chosen as the relay node. To calculate $f_G(g)$, we need to calculate the probability that the distance gain is in a small range of $[g, g+\Delta g]$. As illustrated in the left part of Figure 4, the whole cell space is divided into three regions: S_1, S_2 and S_3. Since the relay node is closer to the base station than any other node falling into the transmission range of the user, there should be no node in S_2 in the left part of Figure 4. To achieve a distance gain of $[g, g+\Delta g]$, there should be at least one node falling into S_3. Since the area of S_3 is proportional to Δg, the probability that two or more nodes fall into S_3 is a higher order of Δg, and thus will be ignored. Therefore, the probability of the distance gain in the range of $[g, g+\Delta g]$ is the probability that when we randomly drop $N-1$ nodes (excluding the user under study) into the cell, one node falls into S_3, no node falls into S_2 and $N-2$ nodes fall into the remaining area S_1. Based on the multinomial distribution:

$$\begin{aligned} f_G(g) &= \lim_{\Delta g \to 0} \frac{\Pr(N-2 \text{ nodes in } S_1, \text{no node in } S_2, \text{one node in } S_3)}{\Delta g}, \\ &= \lim_{\Delta g \to 0} \frac{(N-1)!}{(N-2)!1!0!} (q_1)^{N-2} (q_2)^0 \frac{q_3}{\Delta g} = \lim_{\Delta g \to 0} (N-1) q_1^{N-2} \frac{q_3}{\Delta g}. \end{aligned} \tag{10}$$

where q_1, q_2, q_3 are the probabilities of users located in the area S_1, S_2, S_3. Due to the uniform distribution of the users, $q_i = \frac{S_i}{S_c}, i = 1, 2, 3$, where S_c is the area of entire cell.

S_2 is the overlapping area of two circles. For two circles with a known distance d_{12} between their centers and with radius of each circle c_1 and c_2, let $S_{II}(d_{12}, c_1, c_2)$ represent their overlapping area. The detailed derivation of $S_{II}(d_{12}, c_1, c_2)$ is available in [22]. For our case, $S_2 = S_{II}(d, r_t, d-g)$. For a fixed r_t, S_2 is a function of g and d, so we use $S_2(g, d)$ from this point on. It is easy to verify that

$$\lim_{\Delta g \to 0} q_1 = 1 - \frac{S_2(g,d)}{S_c} = 1 - \frac{S_{II}(d, r_t, d-g)}{S_c}, \tag{11}$$

$$\lim_{\Delta g \to 0} \frac{q_3}{\Delta g} \cdot S_C = \frac{S_3}{\Delta g} = -\frac{\mathrm{d}S_2(g,d)}{\mathrm{d}g} = \frac{\mathrm{d}S_{II}(d, r_t, x)}{\mathrm{d}x}|_{x=d-g}. \tag{12}$$

Consequently, we have

$$f_G(g,d) = \frac{N-1}{S_c} \cdot \left(1 - \frac{S_{II}(d, r_t, d-g)}{S_c}\right)^{N-2} \cdot \frac{\mathrm{d}S_{II}(d, r_t, x)}{\mathrm{d}x}|_{x=d-g}. \tag{13}$$

The expected one-hop distance gain for a user at a distance d from the base station can be derived as:

$$\mu_G(d) = \int_0^{r_t} g f_G(g,d)\mathrm{d}g. \tag{14}$$

1) Distance Gain Using Two-hop Relay: The way to derive the distance gain in the two-hop case is similar to the one-hop case. However the two hop case is computationally more complex. To accurately characterize the two-hop relay gain, we need to calculate the joint density of the distance gain of the first and second relay hop. As illustrated in the right part of Figure 4, let g_1 be the distance gain of the first-hop relay, θ be the angle between the first-hop helper and the user with the base station as the origin, g_2 be the distance gain of the second-hop relay. In a manner similar to the one-hop case, we can calculate the joint density function $f(g_1,\theta,g2)$ by calculating the multinomial distribution of $N-1$ nodes fall into five regions as illustrated in the right part of Figure 4. Let n_i be the number of nodes falling into area S_i. We need to calculate the multinomial probability of $n_1 = N-3, n_2 = n_4 = 0, n_3 = n_5 = 1$. The areas of $S_{1\sim5}$ are functions of g_1, g_2, d and θ.

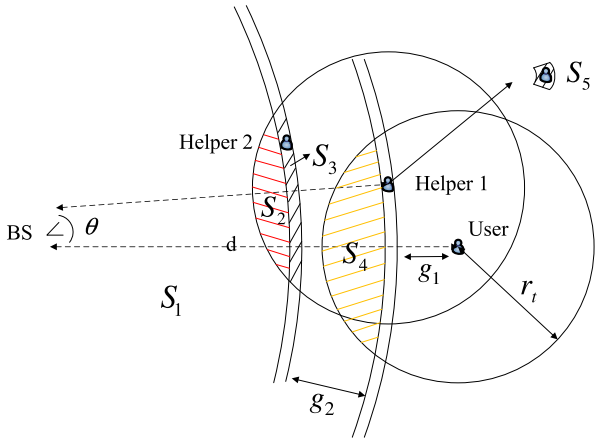

Fig. 4. The two-hop ad-hoc data relay of an arbitrary user

The pdf of the joint distance gain can be calculated as:

$$f(g1,g2,\theta) = \lim_{\Delta g_1,\Delta\theta,\Delta g_2\to 0} \frac{(N-1)(N-2)}{S_c^{N-1}} \cdot S_1^{N-3} \cdot \frac{S_3}{\Delta g_2} \cdot \frac{S_5}{\Delta g_1 \Delta\theta}. \tag{15}$$

It can be determined that $S_5 = (d-g_1)\Delta\theta\Delta g_1$ and $S_1 = S_c - \sum_{i=2}^{5} S_i$. Unfortunately, the calculation of S_2, S_3 and S_4 is fairly involved.

Now let's take a closer look at the positions of the user, helper 1 and helper 2 in Figure 5. Note that the center positions and the radii of the circles C_A, C_B, C_C and C_D can be computed based on g_1, g_2, d, r_t and θ. Going forward $S_{II}(C_i, C_j)$ as the overlapping area of two circles C_i and C_j, $S_{III}(C_i, C_j, C_k)$ as the overlapping area of the three circles C_i, C_j and C_k. i, j and k are chosen from A, B, C, D in the example used herein. With known radii and center positions, the closed formulas of $S_{II}(\cdot)$ and $S_{III}(\cdot)$ are derived in [22].

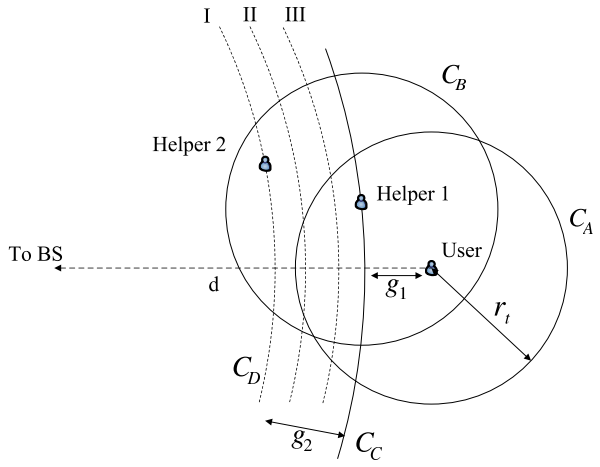

Fig. 5. Reference Figure for positions of the user, helper 1 and helper 2. We label the circles as C_A, C_B, C_C and C_D, with C_A and C_B centered at the user and helper 1, C_C and C_D centered at the Base Station. I, II and III indicate the three different patterns that C_D intersect with C_A and C_B.

With different positions of the helper 2, the C_D may intersect with C_A and C_B in three patterns shown in Figure 5. Here the results are given directly:

case I:

$$S_2 = S_{II}(C_B, C_D), \qquad \frac{dS_3}{dg_2} = -\frac{\mathrm{d}S_2}{\mathrm{d}g_2}, \qquad S_4 = S_{II}(C_A, C_C) \tag{16}$$

In case II and III, S_2 and S_4 overlaps with each other and combine into one part, S_{24}.

case II:

$$\begin{aligned} &\frac{dS_3}{dg_2} = -\frac{\mathrm{d}[S_{II}(C_B, C_D) - S_{II}(C_A, C_D)]}{\mathrm{d}g_2} \\ &S_{24} = S_{II}(C_B, C_D) + S_{II}(C_A, C_C) - S_{II}(C_A, C_D) \end{aligned} \tag{17}$$

case III:

$$\begin{aligned} &\frac{dS_3}{dg2} = -\frac{\mathrm{d}[S_{II}(C_B, C_D) - S_{III}(C_A, C_B, C_D)]}{\mathrm{d}g_2} \\ &S_{24} = S_{II}(C_B, C_D) + S_{II}(C_A, C_C) - S_{III}(C_A, C_B, C_D) \end{aligned} \tag{18}$$

The joint pdf can now be calculated as

$$f(g1, g2, \theta) = \frac{(N-1)(N-2)}{S_c^{N-1}} \cdot S_1^{N-3} \frac{dS_3}{dg_2} \cdot (d - g_1), \tag{19}$$

with different S_1 and $\frac{dS_3}{dg_2}$ as shown from (16) to (18). In case I, $S_1 = S_c - S_2 - S_4$. And in case II and III, $S_1 = S_c - S_{24}$. Finally, the expected two-hop distance gain for user at the distance d can be calculated as

$$\begin{aligned} \mu_{G_1+G_2}(d) &= \int_0^{g_2^{**}} \Phi_{(III)}(g1, g2, d, \theta)\mathrm{d}g_2 \\ &+ \int_{g_2^{**}}^{g_2^{*}} \Phi_{(II)}(g1, g2, d, \theta)\mathrm{d}g_2 + \int_{g_2^{*}}^{r_t} \Phi_{(I)}(g1, g2, d, \theta)\mathrm{d}g_2 \end{aligned} \tag{20}$$

with

$$\Phi_{(i)}(g1, g2, d, \theta) = \int_0^{r_t} \int_{-\theta^*}^{\theta^*} (g_1 + g_2) f_{G_1 G_2 (i)}(g1, g2, d, \theta)\mathrm{d}\theta \mathrm{d}g_1, \ \ i = I, II, III \tag{21}$$

The critical values of g_2 from case I to II and case II to III are defined as g_2^* and g_2^{**}. Moreover, according to the law of consines, we have:

$$\theta^* = \arccos \frac{d^2 + (d - g_1)^2 - r^2}{2d(d - g_1)} \tag{22}$$

B. Impact of ad-hoc wireless relay to user performance

With the concept of "distance gain", we can think of more users moving closer to the base station and "appear to exist" within certain distance of the base station compared to the scenario with no ad-hoc relay. The benefit it brings to our layered video multicast is that the video layers can be received by more users, which have shown in the previous sections. Next we will analytically derive the number of users that effectively move closer to the base station with the aid of ad-hoc wireless relay.

Based on the model we build up, our objective is to calculate on average how many users outside a given distance d can move into the circle, with the aid of ad-hoc relay. If we suppose that different video layers are transmitted with different ranges, such increase represents the number of additional users that can receive a certain video layer. So it has a significant practical meaning.

In detail, we divide the ring between a distance d and $d + r_t$ into many concentric rings, each with a width of $\triangle$. Note that r_t is the range of ad-hoc transmission. One-hop ad-hoc relay is considered in this case; however the approach can be applied to the multiple hop relay scenario. N is the total number of multicast users in the entire cell, and D is the radius of the cell. The average number of users in the kth ring is:

$$N_k(\triangle) = N \cdot \frac{\pi[(d + k\triangle)^2 - (d + (k-1)\triangle)^2]}{\pi D^2} = N \frac{\triangle[(2k-1)\triangle + 2d]}{D^2}. \tag{23}$$

Then, the probability that a user in the k-th ring can move within distance d is:

$$p_k(\triangle) = \int_{k\triangle}^{r_t} f_G(g, d)\mathrm{d}g$$

The average number of users that moves into the circle of radius d is:

$$N_{ave} = \sum_{k=1}^{\lfloor \frac{r_t}{\triangle} \rfloor} N_k(\triangle) \cdot p_k(\triangle). \tag{24}$$

As $\triangle \to 0$, Equation (24) can be rewritten as:

$$N_{ave}(d) = \int_0^{r_t} \frac{2N(d+r)}{D^2} \int_r^{r_t} f_G(g,d)\mathrm{d}g\mathrm{d}r. \tag{25}$$

Recall in our formulation (2), with the assistance of the ad-hoc network, the base station can reach a larger number of users $f(r_i) = f_{BS}(r_i) + f_{AD-HOC}(r_i)$. Now $f_{AD-HOC}(r_i)$ can be approximated by $N_{ave}(d_i)$, where d_i, the distance for certain transmission rate r_i, is discussed and derived in section III-B.

C. Numerical Results Using the Analytical Model

Based on the analytical model presented above, we numerically computed the resulting *distance gain* and *user number increase*. Since the pdf $f_G(g,d)$ is a function of d, the user achieves different distance gain when its distance to the base station varies. The results in this section are for different node densities in a 3G cell with a radius 1000 meters. We set the ad-hoc range at 100 meters. Therefore, if there are a totally 500 nodes, on average each node has $500 \cdot \frac{\pi 100^2}{\pi 1000^2} = 5$ neighbors.

Figure 6 shows how the distance gain g derived in section IV-A and IV-A1 changes with d when TTL is set to one and two. For example, when the total number of multicast users is 700, for the user at the boundary of the cell, i.e, $d = 1000$, the expected one-hop and two-hop distance gains are $g_{TTL=1} = 62.86$ and $g_{TTL=2} = 121.61$.

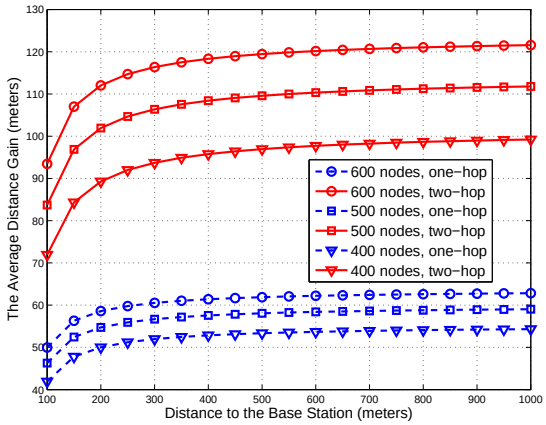

Fig. 6. The one-hop and two-hop Distance Gain for nodes with different distance to the base station.

For the same setting with 500 multicast users, we calculate the increase in the numbers of users at different ranges according to Equation (24). For $d = 500, 700$ and 900 meters, the "number increase/original number of users" are $28.57/125, 38.32/245, 48.08/405$ respectively. Note without ad-hoc, the original number of users goes proportional to d^2 due to the uniform user distribution. We can observe an obvious increase as ad-hoc relay squeezes the users towards the base station. This explains the potential of video quality improvement by using ad-hoc network in the SV-BCMCS protocol.

V. Performance Evaluation

In this section, the performance of SV-BCMCS is evaluated using OPNET based simulations. Compared to the popular network simulators ns-2 and Omnet++ which are free, OPNET is a commercial network simulator using standards based models [23]. The performance of SV-BCMCS is compared with the performance of traditional 3G BCMCS under various scenarios. The impact of node density, node mobility, number of relay hops and the base layer video rate is investigated. Results demonstrate that SV-BCMCS consistently out-performs BCMCS with or without the aid of ad-hoc data relay.

A. Simulation Settings

1) Network Settings: SV-BCMCS is simulated using the wireless modules of OPNET modeler. It is assumed that all multicast users/nodes have two wireless interfaces: one supports a CDMA2000/BCMCS channel for 3G video service, and the other supports IEEE 802.11g for ad-hoc data relay. The data rate of the ad-hoc network is set to be 54 Mb/s, and the transmission

TABLE II
RATE (KB/S) AND PSNR (DB) VALUES OF ALL THE LAYERS FOR THE THREE SVC ENCODED VIDEO SEQUENCES

	Mobile		Football		Bus	
	Rate	PSNR	Rate	PSNR	Rate	PSNR
Base layer	149.1	31.1756	136.0	30.0436	138.5	31.2975
Enh. layer 1	237.5	31.9141	233.5	30.8987	217.3	31.9257
Enh. layer 2	320.2	32.8918	353.5	32.8803	319.8	33.3549
Enh. layer 3	391.8	33.9392	421.1	34.0621	422.0	35.3183
Enh. layer 4	461.1	35.4830	506.4	36.1888	494.3	37.4306
Enh. layer 5	522.0	37.1488	541.6	37.0958	545.1	39.1810

power covers 100 meters. Since OPNET modeler does not provide built-in wireless modules with dual interfaces, the 3G downlink is simulated as if individual users generate their own 3G traffic according to the experimental data presented in [1], [24]. The free-space path loss model is adopted for 3G downlink channels, where the Path Loss Exponent (PLE) is set to be 3.52, and the received thermal noise power is set to be -100.2dBm. Eleven PHY data rates are supported according to the 3GPP2 specifications [25].

The 3G cell is considered to be a circle with a radius of 1000 meters, with a base station located in the center. It is assumed that 3G BCMCS supports a physical layer rate of 204.8 kb/s, which is able to cover the entire cell using a $(32, 28)$ Reed-Solomon error correction code, according to [1]. In our simulation, the transmission power of the 3G base station is set accordingly so that BCMCS can broadcast the video to the entire cell. The same base station transmission power is used in SV-BCMCS evaluations. The users' average PSNR is used as the metric of their received video quality.

2) Scalable Video Settings: Three standard SVC test video sequences, *Mobile*, *Football* and *Bus* in QCIF resolution (176×144 pixels) with a frame rate of 15 frames/sec are used in the simulations. All of the sequences are available from [26]. They are played repeatedly to yield video sequences with a length of approximately 90 seconds. Unless indicated otherwise, the video length is the simulation length for most of our simulation runs. We use JSVM 9.19.7 reference software to encode the video sequences into one base layer and five SVC fidelity enhancement layers with MGS (Medium-Grain fidelity Scalability), based on the SVC extensions of H.264/AVC [4]. In our setting, one GOP (Group-Of-Picture) includes 16 frames. By adjusting the quantization parameters (QP) for each layer in the encoding, all videos are encoded at the rate of about 530 kb/s. The resulting rate points and PSNR values for the layers of each encoded video sequences are summarized in the Table II.

The generated packet information of each video sequence is integrated into OPNET Modeler to simulate video transmission and reception. Since we have modeled interference in OPNET, there will be dynamic packet loss in the ad-hoc network. Thus the video layers are encoded independently using $(6, 5)$ FEC to combat the packet loss, as described in Section III-D2. On the receiving side, a user device decodes an enhancement layer if it has successfully received enough parity packets of this layer, otherwise this layer and all the higher enhancement layers are discarded due to the decoding dependency. Finally we use JSVM to decode the received stream for each user and measure the PSNR of the reconstructed video.

Note that although we can use any general non-decreasing utility function $U(\cdot)$, for simplicity, in our simulation we characterize the video stream by a set of PSNR points u_l, which represent the PSNR of the encoded video with $r_l^{enc} = \sum_{i=1}^{l} R_i$ being the corresponding encoding rate of the scalable video stream at layer $l, l \in 1 \dots L$. Then we solved the optimal resource allocation problem in the simulation with this model. The u_l's and r_l^{enc}'s are as listed in Table II.

B. Stationary Scenarios

In stationary scenarios, a certain number of fixed nodes (users) are uniformly distributed in the 3G cell. The presented results are averages over ten random topologies. The 90% confidence interval is also determined for each simulation point.

1) The Impact of Node Density: In this scenario, we use the settings described in the previous section. The number of multicast receivers in the cell is ranging from 100 to 600, to simulate a sparse to dense node distribution. As a comparison, "Traditional BCMCS" or "BCMCS" indicate the transmission of a single layer video, which we encode using JSVM single-layer coding mode. We encode the single-layer video into approximately 185 kb/s (Specifically, 180.6 kb/s for *Mobile*, 184.9 kb/s for *Football* and 191.3 kb/s for *Bus*). The rate is close to the maximum rate allowed by the BCMCS with the physical layer rate of 204.8 kb/s. The average PSNR for scenarios without an ad-hoc network, and scenarios with ad-hoc network (TTL set to 3) for all three video sequences, are given in Figure 7 and Figure 8.

With and without ad-hoc data relay, SV-BCMCS consistently out-performs the traditional BCMCS. Without ad-hoc relay, SV-BCMCS provides approximately 0.8 dB (*Mobile* sequence), 0.6 dB (*Football* sequence) and 0.2 dB (*Bus* sequence) gain, respectively. The ad-hoc relay leads to extra performance gain. For example, for video sequence *Bus*, when the number of multicast receivers is 100, the ad-hoc relaying gives a 0.36 dB additional PSNR improvement. When the receiver number is

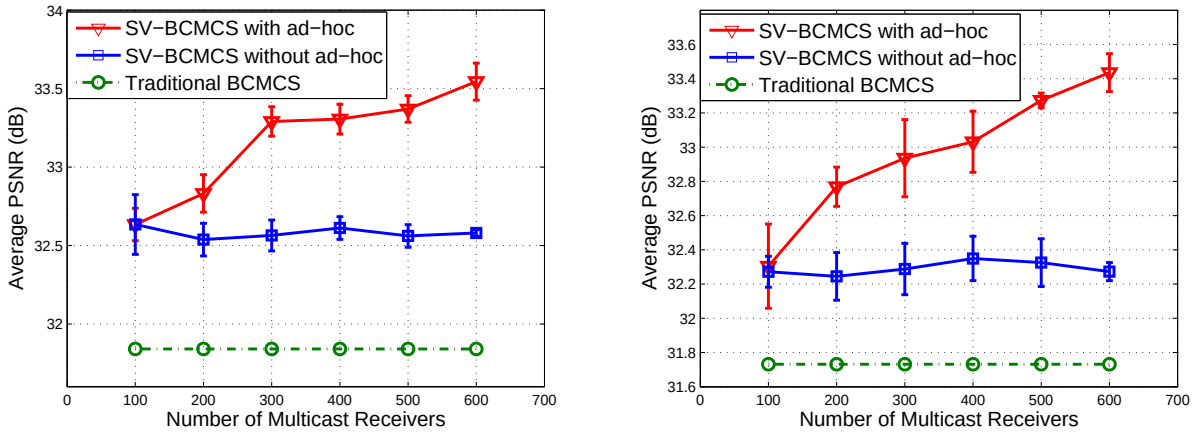

Fig. 7. Impact of number of users (a) Video sequence *Mobile* (b) Video sequence *Football*.

600, the additional improvement reaches 1.17 dB. In general, the PSNR gain with ad-hoc relay increases as the number of users grows because more users facilitate ad-hoc relaying compared to the traditional BCMCS with 600 users, SV-BCMCS improves the users' average PSNR by 1.70 dB for *Mobile sequence*, and 1.70 and 1.35 dB for *Football* and *Bus* sequences respectively.

2) The impact of number of relay hops (TTL): Figure 9 depicts the performance of SV-BCMCS under different TTLs. The analysis in Section IV studies the users' effective distance gain with the aid of ad-hoc data relay. Here the impact of ad-hoc relay is examined in a more practical setting: in the presence of wireless interference and using real video sequences. The experiments are done with the number of users set to be 500.

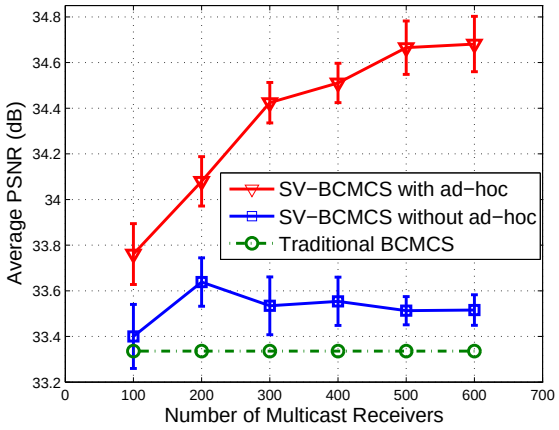

Fig. 8. Impact of number of users (Video sequence *Bus*).

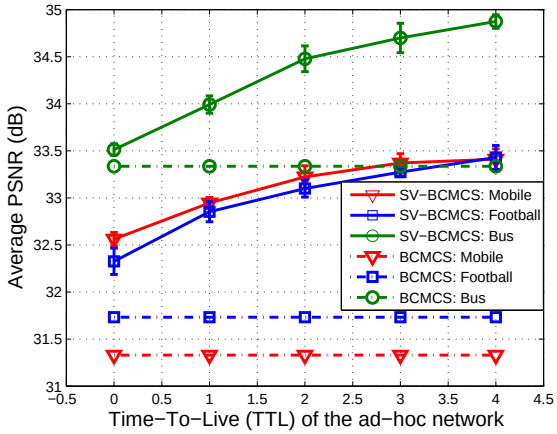

Fig. 9. Impact of TTL on the average PSNR.

As shown in the figure, the performance of SV-BCMCS improves as TTL increases. With more relaying hops, users can potentially connect to the helpers closer to the 3G BS, thus obtaining more higher enhancement layers via ad-hoc relaying. For example, in the figure of *Bus* sequence, with TTL = 1, the average PSNR is about 0.66 dB higher than that in the traditional BCMCS. Such an improvement increases to 1.54 dB when the TTL reaches four. A similar trend can be observed for the *Mobile* and *Football* sequences as well. However, as the TTL becomes larger, the additional interference and communication overhead grow. Hence the PSNR curves flatten out gradually. Finally, note that even with TTL = 0, i.e., without ad-hoc relay, the SV-BCMCS still out-performs BCMCS due to the employment of SVC coding and the optimal resource allocation.

C. Mobile Scenarios

The impact of user mobility to the users' received video quality, represented by PSNR, is studied next. The random walk model with reflection [27] is used to drive the user movement in the simulation. The individual user's moving speed is randomly selected in the range from zero to *maxspeed* (m/s), where *maxspeed* is a simulation parameter. Both moving speed and moving direction are adjusted periodically, with the time period drawn from a uniform distribution between zero and 100 seconds.

TABLE III
IMPACT OF RECONFIGURATION INTERVAL ON THE AVERAGE PSNR (*maxspeed*=10 M/S)

Reconfiguration Interval (sec)	45	30	10	5
Users' Average PSNR (dB)	32.498	32.569	32.697	32.783

We only present the results for the *Mobile* sequence however similar observations are made for other video sequences. Also we loop the video into a longer sequence with a length of 10 minutes. The mobility affects SV-BCMCS's performance in the following two ways: (i) the efficiency of ad-hoc network degrades due to the link failures caused by mobility, and (ii) the optimal channel allocation is disrupted since the user positions keep changing. SV-BCMCS periodically reconfigures the optimal allocation so as to adapt to the user position change.

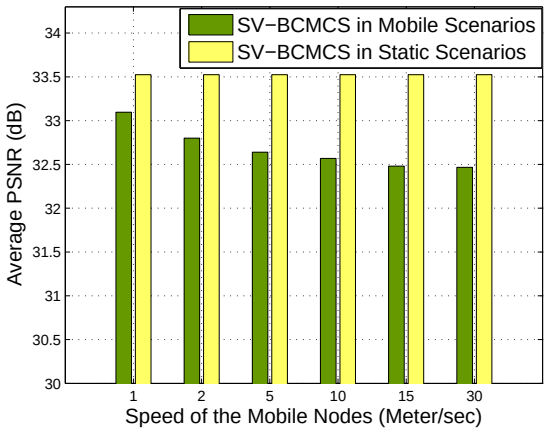

Fig. 10. Impact of *maxspeed* on the average PSNR.

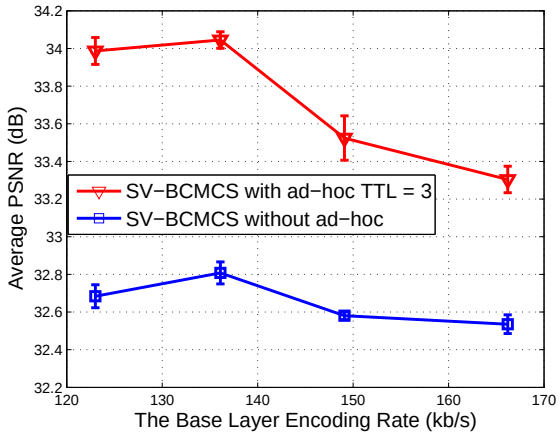

Fig. 11. Impact of base layer encoding rate.

1) The Impact of moving speed: There are 600 users in the cell, with ad-hoc relay hops (TTL) set to be three. The *maxspeed* is set at 1, 2, 5, 10, 15 and 30 m/s, respectively. The base station reconfiguration interval of the optimal channel allocation is set to be 30 seconds. Figure 10 depicts the users' average PSNR for different *maxspeed*. Clearly, the performance of the SV-BCMCS degrades as the users move faster, especially when the speed increases beyond 5 m/s. In fact, when the speed is above 5 m/s, the users' average PSNR is approaching the value without the aid of ad-hoc data relays, as shown in Section V-B.

2) The Impact of the Reconfiguration Interval: Table III summarizes the impact of optimal allocation reconfiguration interval on the average PSNR when *maxspeed* is 10 m/s. As the interval becomes shorter, the SV-BCMCS can adapt to the mobile environment faster, leading to better performance. This is at the price of computational power, communication overhead, and changing video quality perceived by some users. Hence the reconfiguration interval should be selected to strike the right balance.

D. Tradeoffs between the Base Layer Rate and the Overall Performance

In SV-BCMCS, depending on a user's location, it may receive the same video at different quality levels by receiving a different number of video layers. In the worst case, a user may only receive the base layer, which is transmitted to the entire cell. SV-BCMCS allows users having better channel condition to receive better quality video, which is fair in the sense of maximizing the aggregate utility for all users. The study of the right fairness metric, however, is outside the scope of this paper. Here we focus on the tradeoffs between the base layer rate and the overall improvement of user perceived video quality.

Figure 11 depicts the average PSNR vs. the base layer rate in SV-BCMCS with and without ad-hoc data relay. The *Mobile* sequence is being used. There are 600 fixed users in the 3G cell. We change the base layer rate by adjusting the QP for the base layer during encoding. The QP for the enhancement layer rate is fixed which gives a relatively similar encoding rate for the enhancement layers. The resulting rates for base layer are 123.0, 136.1, 149.1 and 166.2 kb/s respectively. We can see that as the base layer rate increases further beyond 136.1 kb/s, the users' average PSNR decreases. The base layer rate must not exceed the single layer rate (204.8 kb/s) as used in BCMCS. Approaching this rate, the entire channel can only transmit the base layer, and there is hardly any difference between SV-BCMCS and BCMCS. Intuitively, the high base rate leaves less "room" for SV-BCMCS to optimize and to achieve a higher average PSNR.

Figure 12 shows the users' average PSNR vs. the distance to the base station in SV-BCMCS. The base layer rate is set to be 149.1 kb/s and 166.2 kb/s respectively and all the other settings are the same as above. Each point in the figure represents one user. Clearly, more users in the small base layer rate case (149.1 kb/s) are able to enjoy higher PSNR than in the large

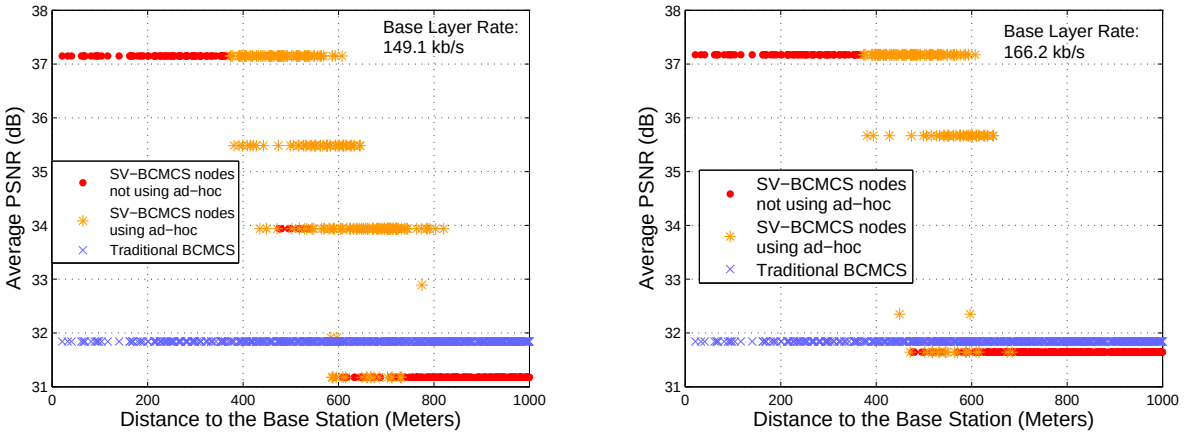

Fig. 12. Tradeoffs of the base layer rate and the overall performance in SV-BCMCS. Optimal resource allocation significantly improves the system-wide video rate at the price of a small quality decrease for nodes close to the boundary; ad-hoc relays further increase the video quality for all users, almost all users achieve a higher video quality than in the traditional BCMCS.

base layer rate case (166.2 kb/s). Specifically, 301 users in the first case are with PSNR more than 32.0 dB, compared with 208 users in the second case. Using less channel bandwidth to deliver a smaller rate base layer enables enhancement layers to be transmitted further. However, the users who only obtain the base layer perceive worse video quality in the small base layer rate case than in the large base layer rate case. With the aid of ad-hoc data relay, more users are able to receive video with higher quality regardless of the base layer rate.

VI. Discussion and Future Work

In this section we discuss several issues relevant to the SV-BCMCS architecture.

Multiple Cells: The technique of soft-combining across multiple cells for EV-DO BCMCS is proved to benefit the edge users by enhancing their data throughput and transmission reliability. Currently we didn't integrate the soft-combining into our optimal resource allocation but only consider the single-cell case. This is left as our future work. With soft-combining enabled, the edge users will experience higher data rate, while the users in the middle of the cell can also have their multicast rate improved due to SV-BCMCS, which leads to a more fair performance.

Opportunistic Receiving: In a real scenario, due to the effect of fading and shadowing, the receiving signal strength varies in a small time scale, which results in variations in channel conditions for each user. For example in Figure 2, it is possible that node A does not receive all the layer 4 packets while node B receives some of the packets from layer 4. Our next step is to model the wireless links as probabilistic which is approaching the reality. In this way, the optimal resource allocation and relay routing will be redesigned accordingly.

Interference in Ad-hoc Network: Interference in the main factor limiting the throughput of multi-hop wireless ad-hoc network. Even without collision, simultaneous transmissions in the same channel will interfere with each other, resulting in the degradation of the link rates. The OPNET-based simulations we conducted already include the interference effect. While simulations give a fairly good performance, it still trails the theoretical bound assuming perfect ad-hoc transmission, due to interference. One of our future work is to optimize the multicast tree in ad-hoc relay network. Such multicast tree guarantees each user still receiving the video layers it should receive decided in resource allocation, while minimizing the network interference.

VII. Conclusion

In this paper we present SV-BCMCS, a novel scalable video broadcast/multicast solution that efficiently integrates scalable video coding, 3G broadcast and ad-hoc forwarding. We formulate the resource allocation problem for scalable video multicast in a hybrid network whose optimal solution can be resolved by a dynamic programming algorithm. Efficient helper discovery and video forwarding schemes are designed for practical layered video/content dissemination through ad-hoc networks. Furthermore, we analyze the effective distance gain enabled by ad-hoc relay, which provides insight into the video quality improvement made possible by using ad-hoc data relay. Finally, OPNET based real video simulations show that a practical SV-BCMCS increases the users' average PSNR by 1.35 $\sim$ 1.70 dB for the video sequences we use, with the ad-hoc networks accounting for around 1.2 dB improvement. Moreover, SV-BCMCS still maintains a minimum of 0.80 dB performance improvement when the nodes' moving speed is less than 5 m/s, while periodical reconfiguration is necessary in fast moving scenarios. The tradeoffs between the base layer rate and the overall performance is discussed and we demonstrate that SV-BCMCS can significantly improve the system-wide video quality, though a few viewers close to the boundary will have a slight quality degradation.

REFERENCES

[1] P. Agashe, R. Rezaiifar, and P. Bender, "CDMA2000 High Rate Broadcast Packet Data Air Interface Design," *IEEE Commun. Mag.*, vol. 42, no. 2, pp. 83–89, February 2004.

[2] J. Wang, R. Sinnarajah, T. Chen, Y. Wei, and E. Tiedemann, "Broadcast and Multicast Services in CDMA2000," *IEEE Commun. Mag.*, vol. 42, no. 2, pp. 76–82, February 2004.

[3] "Third Generation Partnetship Project (3GPP2)." [Online]. Available: http://www.3gpp2.org/

[4] H. Schwarz, D. Marpe, and T. Wiegand, "Overview of the Scalable Video Coding Extension of the H.264/AVC Standard," *IEEE Trans. Circuits Syst. Video Technol.*, vol. 17, no. 9, pp. 1103–1120, September 2007.

[5] H. Luo, R. Ramjee, P. Sinha, L. E. Li, and S. Lu, "UCAN: A Unified Cellular and Ad-Hoc Network Architecture," in *Proc. of ACM MOBICOM*, 2003.

[6] H. Hsieg and R. Sivakumar, "On Using Peer-to-Peer Communication in Cellular Wireless Data Networks," *IEEE Trans. Mobile Comput.*, vol. 3, no. 1, pp. 57–72, February 2004.

[7] J. C. Park and S. K. Kasera, "Enhancing Cellular Multicast Performance Using Ad Hoc Networks," in *Proc. of IEEE Wireless Comm. and Networking Conf. (WCNC)*, 2005.

[8] R. Bhatia, L. E. Li, H. Luo, and R. Ramjee, "ICAM: Integrated Cellular and Ad Hoc Multicast," *IEEE Trans. Mobile Comput.*, vol. 5, no. 8, pp. 1004–1015, August 2006.

[9] K. Sinkar, A. Jagirdar, T. Korakis, H. Liu, S. Mathur, and S. Panwar, "Cooperative Recovery in Heterogeneous Mobile Networks," in *Proc. of IEEE SECON*, 2008.

[10] C.-S. Hwang and Y. Kim, "An Adaptive Modulation Method for Multicast Communications of Hierarchical Data in Wireless Networks," in *Proc. of IEEE International Conf. on Commun. (ICC)*, 2002.

[11] J. Shi, D. Qu, and G. Zhu, "Utility Maximization of Layered Video Multicasting for Wireless Systems with Adaptive Modulation and Coding," in *Proc. of IEEE International Conf. on Commun. (ICC)*, 2006.

[12] J. Kim, J. Cho, and H. Shin, "Layered Resource Allocation for Video Broadcasts over Wireless Networks," *IEEE Trans. on Consumer Electronics*, vol. 54, no. 4, pp. 1609–1616, November 2008.

[13] P. Li, H. Zhang, B. Zhao, and S. Rangarajan, "Scalable video multicast in multi-carrier wireless data systems," in *Network Protocols, 2009. ICNP 2009. 17th IEEE International Conference on*, 2009.

[14] D. Hu, S. Mao, Y. Hou, and J. Reed, "Scalable video multicast in cognitive radio networks," *Selected Areas in Communications, IEEE Journal on*, vol. 28, no. 3, pp. 334 –344, april 2010.

[15] T. Schierl, S. Johansen, A. Perkis, and T. Wiegand, "Rateless scalable video coding for overlay multisource streaming in manets," *J. Vis. Commun. Image Represent.*, vol. 19, no. 8, pp. 500–507, 2008.

[16] S. Hua, Y. Guo, Y. Liu, H. Liu, and S. Panwar, "Sv-bcmcs: Scalable video multicast in hybrid 3g/ad-hoc networks," in *Global Telecommunications Conference, 2009. GLOBECOM 2009. IEEE*, nov. 2009.

[17] K. Stuhlmuller, N. Farber, M. Link, and B. Girod, "Analysis of video transmission over lossy channels," *Selected Areas in Communications, IEEE Journal on*, vol. 18, no. 6, pp. 1012 –1032, 2000.

[18] H. Zhang, Y. Zheng, M. Khojastepour, and S. Rangarajan, "Scalable video streaming over fading wireless channels," in *Wireless Communications and Networking Conference, 2009. WCNC 2009. IEEE*, 2009.

[19] M. van der Schaar, S. Krishnamachari, S. Choi, and X. Xu, "Adaptive cross-layer protection strategies for robust scalable video transmission over 802.11 wlans," *Selected Areas in Communications, IEEE Journal on*, vol. 21, no. 10, pp. 1752 – 1763, dec. 2003.

[20] W.-T. Tan and A. Zakhor, "Video multicast using layered fec and scalable compression," *Circuits and Systems for Video Technology, IEEE Transactions on*, vol. 11, no. 3, pp. 373 –386, mar 2001.

[21] S. Mao, S. Lin, S. Panwar, Y. Wang, and E. Celebi, "Video transport over ad hoc networks: multistream coding with multipath transport," *Selected Areas in Communications, IEEE Journal on*, vol. 21, no. 10, pp. 1721 – 1737, dec. 2003.

[22] M. Fewell, "Area of Common Overlap of Three Circles," Tech. Rep. DSTO-TN-0722, 2006. [Online]. Available: http://hdl.handle.net/1947/4551

[23] "OPNET." [Online]. Available: www.opnet.com

[24] P. Bender, P. Black, M. Grob, R. Padovani, N. Sindhushayana, and A. Viterbi, "CDMA/HDR: A Bandwidth Efficient High Speed Wireless Data Servicefor Nomadic Users," *IEEE Commun. Mag.*, vol. 38, no. 7, pp. 70–77, July 2000.

[25] "CDMA2000 High Rate Broadcast-Multicast Packet Data Air Interface Specification," *3GPP2 Specifications, C.S0054-A_v1.0_060220*, February 2006.

[26] "SVC test sequences." [Online]. Available: ftp.tnt.uni-hannover.de/pub/svc/testsequences

[27] T. Camp, J. Boleng, and V. Davies, "A Survey of Mobility Models for Ad Hoc Network Research," *Wireless Communications and Mobile Computing (WCMC)*, vol. 2, no. 5, pp. 483–502, 2002.